NASA Technical Paper 2386

February 1985

NASA-TP-2386 19850008560

A Cockpit-Display Concept for Executing a Multiple Glide-Slope Approach for Wake-Vortex Avoidance

Terence S. Abbott

NASA

NASA Technical Paper 2386

1985

A Cockpit-Display Concept for Executing a Multiple Glide-Slope Approach for Wake-Vortex Avoidance

Terence S. Abbott

Langley Research Center
Hampton, Virginia

National Aeronautics and Space Administration

Scientific and Technical Information Branch

Summary

A piloted simulation study was undertaken to determine the feasibility of utilizing a forward-looking display to provide information that would enable aircraft to reduce their in-trail separation interval, and hence increase airport capacity, through the application of multiple glide-path approach techniques. Although airport capacity is a direct function of aircraft interarrival separation, this interarrival separation is primarily dictated by wake-vortex considerations. By providing the following aircraft with a higher approach path, reduced-separation approaches may be possible with minimum vortex hazard. The primary objective of this study, then, was to determine whether information could be satisfactorily provided on a forward-looking display to permit the pilot to conduct a multiple glide-slope approach while maintaining a prespecified in-trail separation interval.

The tests were conducted in a motion-base cockpit simulator configured as a current-generation transport aircraft. The dynamic effects of the vortices generated by the lead aircraft were also included in the simulation. The information provided included typical aircraft guidance information and the current and past positions of the lead aircraft. Additionally, the displayed information provided self-separation cues that allowed the pilot to maintain separation on the lead aircraft while performing an instrument approach to landing. Performance data and pilot subjective ratings and comments were obtained during the tests.

The results of this study indicate that multiple glide-slope approaches, procedurally designed for vortex avoidance, are possible while maintaining pilot work load and performance within operationally acceptable limits. In general, then, it would seem that multiple glide-slope approaches are possible even under reduced in-trail separation conditions if the pilot is provided with adequate situational information.

Introduction

The primary factor governing aircraft longitudinal separation within the terminal area during Instrument Flight Rules (IFR) conditions is consideration of the wake-vortex hazard. Over the years, various approaches to the wake-vortex problem have been, and are being, studied, including vortex alleviation, vortex dissipation, and vortex avoidance. A promising technique directed toward vortex avoidance was the so-called multiple glide-slope concept, which provided for the simultaneous use of two or more approach paths lying in the same vertical plane to a given runway. This would be achieved either by having paths of differing glide slopes that intersected the runway at the same point or by retaining the same glide slopes with a difference in the intersection point, or a combination of the two. The idea was based on the fact that during visual conditions, pilots are able to avoid vortex encounters while operating at reduced separation by flying a path that is offset from that of the preceding aircraft. It was clear, however, that application of this concept under instrument conditions would be fraught with situational awareness problems such as, for example, how the pilot would be assured that the preceding aircraft had not strayed from its designated path. With the advent of Cockpit Display of Traffic Information (CDTI) technology, however, it appeared that these situational awareness problems might be overcome.

Although the multiple glide-path approach technique is not a new idea, its implementation has not been initiated because of several possible operational problems associated with it. The primary problems are as follows: interference of the navigation signal, lack of adequate missed-approach guidance, communication interference and delay (delayed go-around instructions, especially critical with reduced separation), and pilot willingness to accept reduced-separation standards. The introduction of the Microwave Landing System (MLS) may reduce or alleviate the navigation-signal interference problem since a microwave system is not as subject to refraction as a conventional instrument landing system (ILS). Additionally, MLS has the potential for resolving many of the missed-approach restrictions via precision-departure guidance. By providing information that would enable the pilot to be responsible for self-separation, the problems associated with communication interference and pilot acceptance may be minimized to a level such that multiple glide-path approaches with reduced separation would be operationally feasible. In seeking methods to improve airport capacity, the question therefore arises as to whether an electronic display, presenting the data-linked position of a lead aircraft, could provide information that would enable the pilot to maintain self-separation under instrument conditions while executing multiple glide-path approaches with reduced separation.

A research effort was undertaken to address this question and to determine the feasibility of this concept. The primary objective of this study was to determine whether information could be satisfactorily provided on a forward-looking, head-up display (HUD) format that would permit the pilot to conduct a multiple glide-slope approach while maintaining a prespecified in-trail separation interval and to monitor adherence of the preceding aircraft with respect to its designated glide path. The operational task was an ILS approach to landing while following a single lead aircraft that was on the same or a lower approach path. During this study, each of three pilots flew 18 approaches with data being taken in the form of quantitative measurements and pilot questionnaires.

Symbols and Abbreviations

AGS	aircraft-guidance symbol
ATC	Air Traffic Control
HUD	head-up display
IAS	indicated airspeed
IAT	interarrival time
IFR	Instrument Flight Rules
ILS	instrument landing system
IMC	instrument meteorological conditions
LOC	localizer
rms	root mean square or quadratic mean
TOGA	takeoff and go-around
ΔT	deviation from nominal time spacing
V_{ref}	nominal final approach speed

Research System

Simulator Description

This study employed the Langley Visual/Motion Simulator (fig. 1), which is a part-task, six-degree-of-freedom, motion-base simulator capable of presenting acceleration and attitude cues to the pilot. Audio cues for aerodynamic buffeting and engine noise were also provided. The aircraft dynamics modeled were those of a Boeing 737 and included nonlinear aerodynamic data and atmospheric effects. Conventional electromechanical navigation instruments, which included a horizontal-situation indicator, a flight director, and distance-measuring equipment (DME), were provided in the cockpit. Neither an autopilot nor a stability augmentation system was provided to the pilot. In addition, no attempt was made to duplicate any specific aircraft cockpit configuration or control-wheel force-feel characteristics. This simulator is further described in reference 1.

Additions to the aircraft force and moment equations caused by the vortex flow fields were made based on a strip-theory technique described in reference 2. The vortices generated by this method were for an aircraft in the normal landing configuration (wing leading- and trailing-edge flaps deployed, all landing flaps at 30°, landing gear down, a lift coefficient of 1.40, and a velocity of 140 knots) and at a weight of 509 914 lb (fig. 2). After generation, the vortices descended at a rate of 6 ft/sec until they reached a point 600 ft below their generation point, at which time they ceased to descend. To simulate ground effect, vortices that came within 60 ft of the ground were held at that altitude and were spread outward at a rate of 6 ft/sec. The lower than nominal vortex descent rate (with nominal being approximately 7 to 8 ft/sec) and the lower than nominal maximum descent position (with nominal being approximately 900 ft below the generation point) were used to provide worse than normal vortex conditions by keeping the vortices closer to the flight path of the generating aircraft.

The visual landing display system (VLDS), shown in figure 3, provides the pilot with an out-the-window color scene of the simulated terrain. The system utilizes a 60- by 24-ft, three dimensionally scaled terrain model, including a large commercial airport, that is traversed in three axes by a gantry carrying a closed-circuit color-television camera. Gantry movements account for aircraft spatial position, whereas the television-probe optics-system motions account for heading, pitch, and bank of the aircraft. Additionally, the capability exists to simulate IMC flight with this system by the employment of a controllable skyplate in its optical probe. Camera and gantry motions are commanded by the aircraft-simulation computer program, and the resulting scene is routed to the window screen of the simulator.

Primary Display Hardware

The primary pilot display for this study employed an "out-the-window" virtual-image system of the beam-splitter, reflective-mirror type. The system, located nominally 50 in. from the pilot's eye, presented a nominal 48° width by 36° height field of view of a 525-line raster video system and provided a 46° by 26° instantaneous field of view. The system supplies a color picture of unity magnification with a resolution on the order of 9 min of arc. The forward-looking, HUD-type presentation for this study was obtained by mixing the video signal from the VLDS camera with the video output from a graphics system by Adage, Inc., which generated the HUD symbology.

Traffic-Generation Technique

The displayed traffic was generated from data previously recorded by using the Langley Flight Simulation Computing Subsystems. Specifically, the traffic data were created by using a piloted simulation capability, in which flights were made along a path that was prescribed by the test scenario. The data from these individual piloted flights were recorded and then, by time correlating, were used as the parameters for the lead aircraft.

Experimental Design

Basic-Display Format

The basic-display format, excluding the traffic information, was the ILS approach portion of the HUD format developed for the McDonnell Douglas MD-80 aircraft family (refs. 3 to 5). Information on this display was made available by the Douglas Aircraft Company, which developed the concept, and Sundstrand Data Control, Inc., which designed and built the HUD equipment. This format was essentially command oriented in that of the three guidance-related symbols (command reference, aircraft guidance, and ILS category II "window"), only the command-reference symbol moved conformally with the external view.

The components of this format, shown in figure 4 with an arbitrary situation, were as follows: The attitude-reference marker, which was a nonmoving symbol, was used in conjunction with the horizon line to indicate pitch attitude and heading. The horizon line and its associated pitch scales moved conformally with the pitch and roll attitudes of the aircraft. Additionally, these scales translated in the roll axis to indicate the drift-correction angle ("crab" angle) of the aircraft. This angle was determined by comparing the course-reference symbol, which was fixed to the horizon line, with the heading symbol, which remained on the horizon line and did not translate with heading. The command-reference symbol was always under the course-reference symbol and would overlay the aiming point on the runway. The aircraft-guidance symbol (AGS) could conceptually be thought of as the position projection of the aircraft being flown. The movement of this symbol, which combines the desired glide-slope angle, the ILS error, and various aircraft position and attitude parameters, is such that by overlaying the command-reference symbol with this symbol, a smooth transition to the glide path will occur and be maintained. The category II ILS window symbol provided a measure of deviation from the nominal glide path and was referenced to the AGS; however, the scaling was not unity and the location of the window symbol was not conformal with the outside view unless the aircraft was flying exactly along the nominal approach path.

It should be noted that the guidance symbology was oriented toward category II ILS approaches. In addition to these attitude and path-guidance symbols, a speed-error symbol was also provided. This symbol grew vertically as a function of speed error, in which a 3-knots-fast indication would show the symbol being above the "wing" line of the AGS and its length being equal to the radius of the center circle of the guidance circle.

The display format was software windowed to provide a 30° wide by 20° high field of view.

Traffic-Display Format

The traffic-display format (fig. 5) was identical to the basic-display format with the addition of three symbols: the present-position symbol of the lead aircraft, the past-position symbol of the lead aircraft, and the numerical symbol for deviation from nominal time spacing. The general concept in the formulation of these symbols was to provide the pilot with adequate information so that he could (1) assess the potential danger stemming from the vortices generated by the lead aircraft, (2) modify his approach profile for vortex avoidance, and (3) adjust his speed to provide for adequate in-trail separation. With this in mind, it was determined that the lateral deviation of the lead aircraft relative to the glide path was of no concern to the follower as long as the lead aircraft remained within nominal ILS limits. For this reason, and while the within-limits condition was met, the lateral position of the lead aircraft was not shown to the follower. The rationale and implementation for each of the symbols are given in the following discussion.

Present-position symbol of lead aircraft. The primary purpose of the present-position symbol of the lead aircraft (L_{present}), which was represented by a left and right "wing," was to provide information to the pilot on how accurately the lead aircraft was following the intended path. This information was important since it was used as the major factor in determining if a missed-approach procedure was required (because of some unusual maneuver of the lead aircraft). This symbol was driven vertically as a function of the ILS glide-slope error of the lead aircraft and was drawn relative to the ILS window symbol. The vertical position was "frozen" once the lead aircraft descended below a 100-ft altitude.

Two lateral motions were also possible with the L_{present} symbol, and these were also based relative to the ILS window symbol. The first motion was a function of the closure rate on the lead aircraft, in which each half of the symbol (the "wings") moved either toward the other (indicating an increase in separation) or farther apart (indicating a decrease in separation). The motion was scaled so that a 20-knot closure rate would reflect as a gap between the circular ends of the symbol and the ILS window-symbol edge and be equal to one-quarter of the width of the ILS window symbol. This closure-rate indication was also limited to 20 knots. The other lateral motion that this symbol could exhibit was a function of the lateral ILS error of the lead aircraft, which would occur only when the error was greater than approximately 1/2°. At this time, the symbol would move laterally as a function of ILS localizer error, with the "wing" opposite the direction of motion being blanked to reduce display clutter. That is, if the lead aircraft were deviating to the right, the right "wing" would move to the right and the left "wing" would be blanked. This feature was important during the last portion of the approach in that the pilot could tell whether the lead aircraft was exiting the runway.

Past-position symbol of lead aircraft. The primary purpose of the past-position symbol of the lead aircraft (L_{past}), which was represented by a left and a right half-circle, was to provide some general information as to where the vortices generated by the lead aircraft were located relative to the following aircraft (referred to as ownship). The implementation of this symbol was a "playback" of the stored position data of the lead aircraft relative to the ILS window symbol of ownship. That is, if ownship were 10 n.mi. from the runway, the L_{past} symbol indicated the position of the lead aircraft relative to the ILS path of ownship when the lead aircraft was also 10 n.mi. from the runway. The horizontal position of the symbol was simply the stored horizontal position of the L_{present} symbol. The vertical position of the symbol was a function of the angular difference between the desired glide-slope angle of ownship and the past, vertical position of the lead aircraft. Since vortices normally descend after generation, the top of each half-circle of the L_{past} symbol was placed on the display at the position that was determined by using the aforementioned technique, thus implying this descending condition. Unlike the L_{present} symbol that "froze" when the lead aircraft descended below 100 ft in altitude, the L_{past} symbol remained active until ownship landed.

Deviation from nominal time-spacing symbol. The numerical symbol denoting a deviation from nominal time spacing (ΔT) was designed to aid the pilot in maintaining the in-trail separation and was an indication, in seconds, of his separation error. The value of ΔT is defined as

$$\Delta T = (\Delta R - T_N V_F)/V_{F,\mathrm{nom}}$$

where ΔR is the in-trail separation, V_F is the ground speed of ownship, $V_{F,\mathrm{nom}}$ is the nominal final approach speed (V_{ref}) of ownship (the final speed that ownship should decelerate to and which is a value selected before the approach begins), and T_N is defined as

$$T_N = T_{\mathrm{desired}} + \frac{R_L}{V_L}\left(1 - \frac{V_{L,\mathrm{nom}}}{V_{F,\mathrm{nom}}}\right)$$

where R_L is the range of the lead aircraft to the runway, V_L is the ground speed of the lead aircraft, T_{desired} is the desired (and preselected) separation time and is calculated as $\Delta R/V_{F,\mathrm{nom}}$ at $R_L = 0$, and $V_{L,\mathrm{nom}}$ is the assumed nominal approach speed of the lead aircraft. The term $\frac{R_L}{V_L}\left(1 - \frac{V_{L,\mathrm{nom}}}{V_{F,\mathrm{nom}}}\right)$ is used to compensate for dissimilar approach speeds. Any error generating from a miscalculation in nominal approach speeds, which are usually based on aircraft type, will diminish as the lead aircraft approaches the runway. For similar final approach speeds, ΔT reduces to

$$\Delta T = \frac{\Delta R - T_{\mathrm{desired}} V_F}{V_{F,\mathrm{nom}}}$$

In addition to the ΔT symbol, which was always over the left side of the AGS, a numeric display of ΔR, displayed in tenths of nautical miles, was displayed over the right side of the AGS at any time that ΔR became less than 2 n.mi. It should be noted that most of the concepts for the traffic-display format, noted previously, were obtained under a contract to Dynasyst, Inc., of Princeton, New Jersey.

One additional modification was implemented in the traffic-display format in an attempt to reduce pilot work load due to the in-trail separation task. This modification involved driving the speed-error symbol on the basic format with a speed-error term obtained from the ΔT equation. Since a zero value of ΔT is the quantity actually desired, we set ΔT equal to 0 and solve for V_F, which is actually, then, the desired V_F (that is, $V_{F,\mathrm{desired}}$) for ΔT equal to 0. Then, the speed error is

$$\text{Speed error} = V_F - V_{F,\mathrm{desired}}$$

Task Description

The basic piloting task in this study was a manual instrument approach and landing while following the vortex-generating lead aircraft in weather conditions simulating a 150-ft ceiling and calm air. The primary approach profile was the ILS approach to runway 26L at the Stapleton International Airport, Denver, Colorado (fig. 6). This approach profile was always used by the lead aircraft and was one of the four approach profiles used by the follower. Three additional profiles were used by the follower and they consisted of a 3° approach angle with an offset touchdown point and two 4.5° approach profiles, one profile with an offset touchdown point and one without. These additional profiles, shown in figure 7, were designed so that the flight path of the follower would always be above the path of the leader during the nonvisual approach portion of the task (fig. 8). The approach-profile configurations were obtained from reference 6. For consistency, a standard pilot-briefing form (see appendix A) was used in briefing each pilot before each simulation session. In addition, the description of initial conditions and performance variables to be measured was given to the test subjects prior to participating in the test. (See appendix B.) The test subjects were further instructed to fly the simulator in a manner that they deemed acceptable for airline-type operations and to avoid radical maneuvers. Besides being professional pilots, the test subjects had attended an airline training school and were experienced in flying Boeing aircraft. During the test runs, the test engineer acted as the copilot in regard to lowering the flaps and other such tasks as directed by the evaluation pilot. The test engineer did not offer comments on the simulated situation during the sessions.

During this study, the pilot was responsible for maintaining a prespecified in-trail interval, either 60 or 45 sec, behind the lead aircraft. The basis for these times was taken from references 7 and 8. The 45-sec interval was the smallest time used (and also, therefore, the smallest separation) since this time borders on the current minimum-possible runway occupancy time (ref. 8).

Traffic Profiles

The traffic scenario utilized in this study was that of a single lead aircraft that was flying the ILS approach to runway 26L at the Stapleton International Airport. Four different profiles for the lead aircraft were used, and they are described in the following discussion.

Profile 1. The first traffic profile was that of an aircraft with $V_{\text{ref}} = 120$ knots (the same as that of ownship). This aircraft flew an almost idle-thrust descent while carefully maintaining the ILS path, landed, and exited the runway in a normal but expeditious manner. This profile was considered the baseline profile.

Profile 2. The second traffic profile was that of an aircraft with $V_{\text{ref}} = 140$ knots (20 knots higher than that of ownship), representing an aircraft in the heavy class. Except for the higher approach speeds, this profile was similar to that of profile 1.

Profile 3. The third profile was exactly the same as that of profile 1 except that the lead aircraft did not exit the runway. This profile was chosen to determine if ownship could detect this type of blunder.

Profile 4. The fourth profile was very similar to that of profile 1 except that when the lead aircraft reached a 150-ft altitude, it executed a missed approach (go-around). This profile, along with profile 3, constituted the two blunder scenarios used in this study.

The glide-slope error, localizer error, and ground-speed profile plots for profiles 1 and 2 are shown in figure 9.

Test Conditions

A total of 54 simulated instrument approaches were flown by three professional pilots to obtain data, with each pilot flying 18 approaches. The test matrix, which is a modified Latin square, is given in table I.

Sufficient training was given both prior to the initial simulation data sessions and before each individual session of the first test section to minimize the learning effects. Except for the two blunder cases, the pilots were trained in all situations shown in the test matrices.

The initial conditions for the lead aircraft were as follows: on the ILS path, approximately 15 n.mi. from the runway threshold, and at an IAS of 250 knots. The initial conditions for ownship were as follows: on the selected ILS path, at an IAS of 250 knots, and at a distance behind the lead aircraft such that ΔT was approximately 0.

Results and Discussion

The results of this study are divided into two areas of discussion. The first section discusses the general results of the study. The second section discusses the effects of the interarrival separation interval, aircraft approach speed, glide-slope offset, glide-slope (GS) angle on runway delivery accuracy (interarrival time and separation), glide-slope tracking performance, and localizer tracking performance. The statistical analysis results of the quantitative data are presented in table II, and the qualitative results from the pilot questionnaires are presented in table III. The data from the blunder scenarios were not used in the analysis of the quantitative data.

General

Traffic situational awareness. All pilots stated that at no time during the study was a problem encountered in understanding the traffic situation. It was stated that the symbolic traffic information was generally intuitive in nature and was, therefore, easy to interpret and use. These results substantiate the findings of a previous work (ref. 9) that utilized the same display format.

Blunder scenarios. During this study, each of the pilots was presented with a potentially hazardous situation, a blunder scenario, in which the lead aircraft either executed a missed approach while on a short final approach or failed to exit the runway after landing. All blunder scenarios were correctly identified by the pilots with the proper corrective action: a go-around maneuver, being initiated before a critical situation could develop. The lead aircraft executing a missed approach was first indicated to the evaluation pilot by the L_{present} symbol moving steadily toward and then above the ILS window symbol. As the L_{present} symbol continued to stay above the ILS-window symbol, and before the L_{past} symbol began to move upward, the pilots always began a go-around maneuver. The occupied-runway blunder became apparent to the evaluation pilot as he approached the runway after the lead aircraft landed by the L_{present} symbol moving neither right nor left, indicating that the lead aircraft was not turning off the runway. The pilots waited until reaching the decision height, and if the lead aircraft was then still on the runway, they would execute a go-around maneuver.

Vortex encounters. At no time during the 54 data runs did a vortex upset occur. This result was obtained (for the flight profiles in which procedurally little or no vertical separation was provided) primarily by the pilot being able to monitor and track the glide-slope precisely and by the fact that the lead aircraft was also, in general, precisely tracking the glide path. Additionally, the fact that a vortex encounter did not occur under these conditions may be attributed, in part, to the pilot's having knowledge of the past position of the lead aircraft and thus being able to stay above that position, thereby reducing the likelihood of an encounter.

Effects of Separation, Speeds, and Glide-Slope Geometry

Glide-slope tracking. The glide-slope tracking error (fig. 10) appears to have a somewhat sinusoidal characteristic. This characteristic is primarily attributed to deployment of the aircraft flaps, which occurs in steps throughout the approach and produces a pitch-attitude change and an increase in lift (for a given speed and angle of attack). Therefore, if ownship were on the glide slope and at the proper pitch attitude required to maintain that flight path prior to flap deployment, the pilot would have to make an immediate and continuous pitch-attitude correction to keep the aircraft on the proper flight path upon and during a flap change. The control technique used by some pilots in this study, however, was to allow the aircraft to begin to trim at the new attitude brought about by a flap change (with a resulting divergence from the glide slope) before initiating a correction to bring the aircraft back to the proper flight path. The reason given for the use of this technique was that it minimized the glide-slope tracking task and reduced the possibility of overcontrolling the aircraft while remaining within acceptable glide-slope limits. With the exception of one approach, the entire ILS path tracking performance was within the category II ILS boundaries. The one exception is described in a subsequent section.

Separation interval. No significant difference (table II) was found between the 60- and 45-sec separation intervals for either the glide-slope or localizer path tracking performance. The pilot work-load rating for the self-separation task, extracted from the pilot questionnaire and shown in table III(c), shows a very slight increase in effort for the 45-sec interval relative to the 60-sec interval. The values of the interarrival separation results are given in figure 11.

Aircraft nominal approach speed. The two nominal approach speeds used in this study by the lead aircraft produced a statistically significant difference in the interarrival separation interval at the 97.5-percent confidence level. The mean interarrival separation interval was approximately 0.02 n.mi. smaller for the 140-knot V_{ref} scenarios relative to the 120-knot V_{ref} scenarios. This difference can be attributed to the compensation term for dissimilar approach speeds in the ΔT computation.

A significant difference was also found for the glide-slope tracking error relative to the nominal approach speeds, with the 140-knot V_{ref} scenario yielding a poorer performance. For similar conditions, the 120-knot V_{ref} scenario produced a mean error of 0.0087° and an rms of 0.0524°, whereas the 140-knot V_{ref} scenario produced a mean error of 0.0425° and an rms of 0.0719°. It should be noted, however, that one of the 140-knot V_{ref} scenarios resulted in a mean glide-slope error that was greater than three times that of any of the other scenarios. The pilot, when questioned immediately after this approach, stated that he thought his performance remained within acceptable limits for the entire approach and that his performance on this approach was not significantly different from that on any of the other approaches. By discounting this particular data run (no. 47, the fifth run in session II for pilot 3), no significant difference was found for the glide-slope tracking error relative to the V_{ref} terms. The pilot subjective ratings indicate that the V_{ref} factor had no effect on work load.

Glide-slope offset. No differences were observed in the performance data between the scenarios involving the no glide-slope offset and the 800-ft offset. Additionally, no differences were noted in the pilot subjective ratings between the glide-slope offsets.

Glide-slope angle. No statistical differences were observed for the runway delivery accuracy factors between the 3° and 4.5° glide-slope angles (fig. 12). No statistically significant differences were observed under similar conditions for the glide-slope error (fig. 10), with mean and rms values of 0.0087° and 0.0473° noted, respectively, for the 3° angle and 0.0087° and 0.0524°, respectively, for the 4.5° angle. A significant difference was obtained, however, for the localizer error (fig. 10), with the 4.5° angle yielding a better performance. Although it would appear from figure 10 that the 3° angle provided better performance relative to path deviation, it should be noted that 83 percent more approaches are shown for the 4.5° angle and that the 4.5°-angle approaches yielded a smaller mean error. For similar conditions, the mean and rms values were 0.1423° and 0.1596°, respectively, for the 3° angle and were 0.0027° and 0.0884°, respectively, for the 4.5° angle.

It should be noted, though, that as the vertical separation interval between the path of ownship and the leader is reduced, the vertical position of ownship moves closer to the vortex flow fields, which appear to the pilot as wind gusts that are ranging in intensity levels from unnoticeable to slight. Since the vortex flow fields interact with the aircraft aerodynamics, an increase in the flow-field strength could result in an increase in the path tracking error. Although no major differences were noted in the pilot subjective ratings between the two glide-slope angles, comments made during several of the 4.5° approaches disclosed that the pilots felt somewhat "uncomfortable"; that is, they felt that it would be extremely difficult, if not impossible, to correct for a higher altitude and faster speed than nominal condition at this approach angle.

Concluding Remarks

A piloted simulation study was undertaken to determine whether information could satisfactorily be provided on a head-up display format that would permit the pilot to conduct a multiple glide-slope instrument approach while maintaining a self-separation interval behind a vortex-generating lead aircraft.

At no time was a problem encountered in understanding the traffic situation. The symbolic traffic information was intuitive in nature and was easy to interpret and use. For the three approaches in which the maneuvering of the lead aircraft would have caused a potentially hazardous condition to occur, the pilots properly identified the condition and initiated an appropriate corrective action.

Under the conditions of this study, multiple glide-slope approaches, procedurally designed for vortex avoidance, were conducted while maintaining pilot work load and performance within operationally acceptable limits. In general, then, it would seem that multiple glide-slope approaches are possible even under reduced in-trail separation conditions if the pilot is provided with adequate situational information.

Langley Research Center
National Aeronautics and Space Administration
Hampton, VA 23665
October 11, 1984

Appendix A

Pilot Briefing

You are the captain of a 737 on a revenue flight. You are expected to comply with all normal ATC speed restrictions and fly the aircraft within its normal performance envelope.

HUD: You are cleared for the approach and landing (normal ATC procedures in effect) with the exception of traffic separation and runway occupancy. <u>You</u> are responsible for these.

Fly as though it were a real operation. NOTE:

(1) $V_{ref} = 120$ knots
(2) Flaps: 0°, 10°, 20°, 25°, 30°, and 40°
(3) Would advise starting with gear down, flaps 0°
(4) The speed brakes are operational.
(5) The TOGA switch is operational.
(6) Lead aircraft with $V_{ref} = 140$ knots are to be considered in the HEAVY class.

Appendix B

Pilot Questionnaire

GLIDE-PATH TRACKING:

(1) Was there any concern with maintaining the aircraft on the glide path?

☐ Yes ☐ No

If yes, what was (or caused) the concern?

(2) Rate the horizontal path-tracking task:

No noticeable work load	Very easy	Easy	Some effort required	Difficult	Very difficult	Impossible

(3) Rate the vertical path-tracking task:

No noticeable work load	Very easy	Easy	Some effort required	Difficult	Very difficult	Impossible

SELF-SEPARATION:

(1) Was there any concern with maintaining a safe separation interval?

☐ Yes ☐ No

If yes, what was (or caused) the concern?

(2) Rate the self-separation task:

No noticeable work load	Very easy	Easy	Some effort required	Difficult	Very difficult	Impossible

(3) Did you accurately maintain the prescribed separation?

☐ Yes ☐ No

If no, why not?

(4) Was the displayed information adequate for safe separation?

☐ Yes ☐ No

If no, why not?

GENERAL:

(1) Was a vortex ever encountered?

☐ Yes ☐ No

If yes, how severe was the encounter and how did it affect the approach?

(2) Was the display information easy to interpret and use?

☐ Yes ☐ No

If no, why not?

(3) General comments:

References

1. Parrish, Russell V.; and Bowles, Roland L.: *Motion/Visual Cueing Requirements for Vortex Encounters During Simulated Transport Visual Approach and Landing.* NASA TP-2136, 1983.
2. Hastings, Earl C., Jr.; and Keyser, Gerald L., Jr.: *Simulator Study of Vortex Encounters by a Twin-Engine, Commercial, Jet Transport Airplane.* NASA TP-1966, 1982.
3. Lowe, J. R.: Improving the Accuracy of HUD Approaches in Windshear With a New Control Law. AIAA Paper 78-1494, Aug. 1978.
4. Lowe, J. R.; and Ornelas, J. R.: Applications of Head-Up Displays in Commercial Transport Aircraft. *Collection of Technical Papers—AIAA 4th Digital Avionics Systems Conference*, Nov. 1981, pp. 409–414. (Available as AIAA-81-2300.)
5. *DC-9 Super 80 Flight Crew Operating Manual—Operating Procedures and Description.* McDonnell Douglas Corp., Dec. 1980, Section 4, 3-10-20, Code 1.
6. Hastings, Earl C., Jr.; and Taylor, Robert T.: *Effects of Landing Approach Methods and Separation Intervals on Single Runway Landing Capacity.* NASA TP-1112, 1977.
7. Swedish, William J.: *Evaluation of the Potential for Reduced Longitudinal Spacing on Final Approach.* Rep. No. FAA-EM-79-7, Aug. 1979. (Available from DTIC as AD A076 434.)
8. Sinha, A. N.; and Haines, A. L.: *Longitudinal Separation Standards on Final Approach for Future* ATC *Environments.* MTR-6979 (Contract No. DOT-FA70WA-2448), MITRE Corp., Oct. 1975.
9. Abbott, Terence S.: *Simulation of a Cockit-Display Concept for Executing a Wake-Vortex Avoidance Procedure.* NASA TP-2300, 1984.

TABLE I. TEST MATRIX

[Standard conditions for leader: 60-sec separation; V_{ref} = 120 knots]

Pilot	Session I				Session II				Session III			
	Test sequence for glide-slope angles of—				Test sequence for glide-slope angles of—				Test sequence for glide-slope angles of—			
	3°	3° (a)	4.5°	4.5° (a)	3°	3° (a)	4.5°	4.5° (a)	3°	3° (a)	4.5°	4.5° (a)
1	1	2	[b]3, 4	[c]5, 6	6	5	3,[d] 4	1,[c] 2	4	3	1,[b] 2	5,[c] 6
2	5	6	3,[d] 4	[c]1, 2	2	1	[b]5, 6	[c]3, 4	3	4	[b]5, 6	[c]1, 2
3	5	6	[b]3, 4	1,[c] 2	2	1	5,[b] 6	3,[c] 4	3	6	[d]4, 5	1,[c] 2

[a]800-ft displaced touchdown zone.
[b]For the leader (1 run), V_{ref} = 140 knots.
[c]45-sec separation (1 run).
[d]Blundering leader (1 run).

TABLE II. STATISTICAL ANALYSIS

[Note 1—Theoretical IAT is the velocity of ownship divided by the range of ownship when the lead aircraft crosses the runway threshold.

Note 2—Actual IAT is the time that ownship crosses the runway threshold minus the time that the lead aircraft crosses the runway threshold.]

** Separation (n.mi.) **

45 sec Separation
All non-blunder runs

Pilot 1	Samples	3	Mean	1.8	Deviation	0.01	Range	0.01	Minimum	1.8	Maximum	1.8
Pilot 2	Samples	3	Mean	1.8	Deviation	0.08	Range	0.16	Minimum	1.7	Maximum	1.9
Pilot 3	Samples	3	Mean	1.8	Deviation	0.00	Range	0.01	Minimum	1.8	Maximum	1.8
Totals	Samples	9	Mean	1.8	Deviation	0.04	Range	0.16	Minimum	1.7	Maximum	1.9

60 sec Separation
3 degree glide-slope angle

Pilot 1	Samples	6	Mean	2.4	Deviation	0.03	Range	0.07	Minimum	2.4	Maximum	2.4
Pilot 2	Samples	6	Mean	2.4	Deviation	0.03	Range	0.08	Minimum	2.4	Maximum	2.5
Pilot 3	Samples	6	Mean	2.4	Deviation	0.01	Range	0.02	Minimum	2.4	Maximum	2.4
Totals	Samples	18	Mean	2.4	Deviation	0.02	Range	0.11	Minimum	2.4	Maximum	2.5

60 sec Separation
4.5 degree glide-slope angle

Pilot 1	Samples	8	Mean	2.4	Deviation	0.01	Range	0.03	Minimum	2.4	Maximum	2.4
Pilot 2	Samples	8	Mean	2.4	Deviation	0.03	Range	0.07	Minimum	2.4	Maximum	2.4
Pilot 3	Samples	8	Mean	2.4	Deviation	0.01	Range	0.03	Minimum	2.4	Maximum	2.4
Totals	Samples	24	Mean	2.4	Deviation	0.02	Range	0.07	Minimum	2.4	Maximum	2.4

TABLE II. Continued

** Theoretical IAT (sec) ** (see note 1)

45 sec Separation
All non-blunder runs

Pilot 1	Samples	3	Mean	45.2	Deviation	0.42	Range	0.76	Minimum	44.7	Maximum	45.5
Pilot 2	Samples	3	Mean	44.8	Deviation	1.39	Range	2.78	Minimum	43.4	Maximum	46.2
Pilot 3	Samples	3	Mean	45.1	Deviation	0.17	Range	0.34	Minimum	44.9	Maximum	45.3
Totals	Samples	9	Mean	45.0	Deviation	0.75	Range	2.78	Minimum	43.4	Maximum	46.2

60 sec Separation
3 degree glide-slope angle

Pilot 1	Samples	6	Mean	60.1	Deviation	0.61	Range	1.81	Minimum	59.1	Maximum	60.9
Pilot 2	Samples	6	Mean	60.2	Deviation	1.59	Range	4.31	Minimum	58.7	Maximum	63.0
Pilot 3	Samples	6	Mean	60.1	Deviation	0.47	Range	1.30	Minimum	59.6	Maximum	60.9
Totals	Samples	18	Mean	60.1	Deviation	0.96	Range	4.31	Minimum	58.7	Maximum	63.0

60 sec Separation
4.5 degree glide-slope angle

Pilot 1	Samples	8	Mean	59.7	Deviation	0.77	Range	2.07	Minimum	58.3	Maximum	60.4
Pilot 2	Samples	8	Mean	59.6	Deviation	0.53	Range	1.64	Minimum	58.9	Maximum	60.5
Pilot 3	Samples	8	Mean	59.8	Deviation	0.29	Range	0.82	Minimum	59.4	Maximum	60.2
Totals	Samples	24	Mean	59.7	Deviation	0.55	Range	2.22	Minimum	58.3	Maximum	60.5

TABLE II. Continued

** Actual IAT (sec) ** (see note 2)

45 sec Separation
All non-blunder runs

Pilot 1	Samples	3	Mean	46.5	Deviation	0.03	Range	0.06	Minimum	46.5	Maximum	46.6
Pilot 2	Samples	3	Mean	46.9	Deviation	2.43	Range	4.83	Minimum	44.3	Maximum	49.2
Pilot 3	Samples	3	Mean	46.7	Deviation	0.20	Range	0.40	Minimum	46.5	Maximum	46.9
Totals	Samples	9	Mean	46.7	Deviation	1.23	Range	4.83	Minimum	44.3	Maximum	49.2

60 sec Separation
3 degree glide-slope angle

Pilot 1	Samples	6	Mean	63.3	Deviation	0.55	Range	1.61	Minimum	62.5	Maximum	64.2
Pilot 2	Samples	6	Mean	62.5	Deviation	1.72	Range	4.61	Minimum	59.4	Maximum	64.1
Pilot 3	Samples	6	Mean	63.5	Deviation	0.29	Range	0.76	Minimum	63.0	Maximum	63.8
Totals	Samples	18	Mean	63.1	Deviation	1.10	Range	4.71	Minimum	59.4	Maximum	64.2

60 sec Separation
4.5 degree glide-slope angle

Pilot 1	Samples	8	Mean	63.0	Deviation	1.26	Range	3.16	Minimum	61.2	Maximum	64.4
Pilot 2	Samples	8	Mean	62.0	Deviation	1.00	Range	2.71	Minimum	60.5	Maximum	63.2
Pilot 3	Samples	8	Mean	63.4	Deviation	0.30	Range	0.85	Minimum	63.0	Maximum	63.8
Totals	Samples	24	Mean	62.8	Deviation	1.08	Range	3.91	Minimum	60.5	Maximum	64.4

TABLE II. Continued

Theoretical IAT - 60 sec separation

Cell means for first dependent variable

Pilots =	Pilot1	Pilot1	Pilot2	Pilot2	Pilot3	Pilot3	marginal
GS angle=	3 degree	4.5 degree	3 degree	4.5 degree	3 degree	4.5 degree	
IAT	60.10667	59.66250	60.11333	59.51375	60.09500	59.80875	59.85167
count	6	8	6	8	6	8	42

Standard deviations for first dependent variable

Pilots =	Pilot1	Pilot1	Pilot2	Pilot2	Pilot3	Pilot3
GS angle=	3 degree	4.5 degree	3 degree	4.5 degree	3 degree	4.5 degree
IAT	0.61076	0.77136	1.58516	0.53034	0.47162	0.28812

Analysis of variance for first
dependent variable - Theoretical IAT

source	sum of squares	degrees of freedom	mean square	f	tail probability
Mean	147538.84571	1	147538.84571	238651.88	0.0000
Pilots	0.13125	2	0.06563	0.11	0.8996
GS angle	2.02160	1	2.02160	3.27	0.0789
Interaction	0.16831	2	0.08415	0.14	0.8732
Error	22.25584	36	0.61822		

TABLE II. Continued

Actual IAT - 60 sec separation

Cell means for first dependent variable

Pilots = GS angle=	Pilot1 3 degree	Pilot1 4.5 degree	Pilot2 3 degree	Pilot2 4.5 degree	Pilot3 3 degree	Pilot3 4.5 degree	marginal
IAT	63.30500	62.94625	62.41333	61.97500	63.45000	63.37750	62.89048
count	6	8	6	8	6	8	42

Standard deviations for first dependent variable

Pilots = GS angle=	Pilot1 3 degree	Pilot1 4.5 degree	Pilot2 3 degree	Pilot2 4.5 degree	Pilot3 3 degree	Pilot3 4.5 degree
IAT	0.55157	1.25977	1.71960	1.00056	0.28761	0.30264

Analysis of variance for first
dependent variable - Actual IAT

source	sum of squares	degrees of freedom	mean square	f	tail probability
Mean	162835.88457	1	162835.88457	165231.65	0.0000
Pilots	11.14521	2	5.57260	5.65	0.0073
GS angle	0.86420	1	0.86420	0.88	0.3553
Interaction	0.25384	2	0.12692	0.13	0.8796
Error	35.47802	36	0.98550		

TABLE II. Continued

Actual IAT - 60 sec separation/same Vref

Cell means for first dependent variable

Pilots =	Pilot1	Pilot1	Pilot2	Pilot2	Pilot3	Pilot3	marginal
Offset =	none	offset	none	offset	none	offset	
IAT	63.16000	63.12333	61.95167	62.56000	63.39667	63.49167	62.94722
count	6	6	6	6	6	6	36

Standard deviations for first dependent variable

Pilots =	Pilot1	Pilot1	Pilot2	Pilot2	Pilot3	Pilot3
Offset =	none	offset	none	offset	none	offset
IAT	1.01978	0.79520	1.63461	1.17976	0.29180	0.31859

Analysis of variance for first
dependent variable - Actual IAT

source	sum of squares	degrees of freedom	mean square	f	tail probability
Mean	142644.70028	1	142644.70028	144505.77	0.0000
Pilots	9.15337	2	4.57669	4.64	0.0176
Offset	0.44444	1	0.44444	0.45	0.5074
Interaction	0.69687	2	0.34844	0.35	0.7055
Error	29.61363	30	0.98712		

TABLE II. Continued

Actual IAT - 60 sec separation/same Vref/4.5 deg GS angle

Cell means for first dependent variable

Pilots =	Pilot1	Pilot1	Pilot2	Pilot2	Pilot3	Pilot3	marginal
Offset =	none	offset	none	offset	none	offset	
IAT	62.96667	62.99000	62.21667	61.98000	63.22333	63.65333	62.83833
count	3	3	3	3	3	3	18

Standard deviations for first dependent variable

Pilots =	Pilot1	Pilot1	Pilot2	Pilot2	Pilot3	Pilot3
Offset =	none	offset	none	offset	none	offset
IAT	1.54571	0.93408	1.14692	1.34748	0.33322	0.15308

Analysis of variance for first
dependent variable - Actual IAT

source	sum of squares	degrees of freedom	mean square	f	tail probability
Mean	71075.81045	1	71075.81045	65333.70	0.0000
Pilots	5.56320	2	2.78160	2.56	0.1189
Offset	0.02347	1	0.02347	0.02	0.8857
Interaction	0.33871	2	0.16936	0.16	0.8575
Error	13.05467	12	1.08789		

TABLE II. Continued

Separation - 60 sec

Cell means for first dependent variable

Pilots =	Pilot1	Pilot1	Pilot2	Pilot2	Pilot3	Pilot3	marginal
GS angle=	3 degree	4.5 degree	3 degree	4.5 degree	3 degree	4.5 degree	
Separation	2.36000	2.36250	2.36667	2.36750	2.37500	2.36625	2.36619
count	6	8	6	8	6	8	42

Standard deviations for first dependent variable

Pilots =	Pilot1	Pilot1	Pilot2	Pilot2	Pilot3	Pilot3
GS angle=	3 degree	4.5 degree	3 degree	4.5 degree	3 degree	4.5 degree
Separation	0.02757	0.01035	0.02944	0.02550	0.00548	0.00916

Analysis of variance for first
dependent variable - Separation

source	sum of squares	degrees of freedom	mean square	f	tail probability
Mean	230.37810	1	230.37810	585259.27	0.0000
Pilots	0.00061	2	0.00031	0.78	0.4657
GS angle	0.00003	1	0.00003	0.09	0.7721
Interaction	0.00025	2	0.00013	0.32	0.7274
Error	0.01417	36	0.00039		

TABLE II. Continued

Separation - 60 sec/same Vref

Cell means for first dependent variable

Pilots =	Pilot1	Pilot1	Pilot1	Pilot1	Pilot2	Pilot2	Pilot2	Pilot2
GS angle=	3 degree	3 degree	4.5 degree	4.5 degree	3 degree	3 degree	4.5 degree	4.5 degree
Offset =	none	offset	none	offset	none	offset	none	offset
Separation	2.62837	2.60315	2.59092	2.62398	2.62962	2.60947	2.61941	2.63032
count	3	3	3	3	3	3	3	3

Pilots =	Pilot3	Pilot3	Pilot3	Pilot3	marginal
GS angle=	3 degree	3 degree	4.5 degree	4.5 degree	
Offset =	none	offset	none	offset	
Separation	2.63676	2.61921	2.62978	2.62605	2.62059
count	3	3	3	3	36

Standard deviations for first dependent variable

Pilots =	Pilot1	Pilot1	Pilot1	Pilot1	Pilot2	Pilot2	Pilot2	Pilot2
GS angle=	3 degree	3 degree	4.5 degree	4.5 degree	3 degree	3 degree	4.5 degree	4.5 degree
Offset =	none	offset	none	offset	none	offset	none	offset
Separation	0.00516	0.03050	0.01083	0.01256	0.01784	0.02001	0.01370	0.00990

Pilots =	Pilot3	Pilot3	Pilot3	Pilot3
GS angle=	3 degree	3 degree	4.5 degree	4.5 degree
Offset =	none	offset	none	offset
Separation	0.00133	0.00308	0.00218	0.00616

Analysis of variance for first dependent variable - Separation

source	sum of squares	degrees of freedom	mean square	f	tail probability
Mean	247.22894	1	247.22894	1295561.41	0.0000
Pilots	0.00165	2	0.00083	4.32	0.0249
GS angle	0.00001	1	0.00001	0.05	0.8267
Offset	0.00013	1	0.00013	0.67	0.4197
Pilots/GS angle	0.00028	2	0.00014	0.74	0.4877
Pilots/Offset	0.00032	2	0.00016	0.84	0.4434
GS angle/Offset	0.00266	1	0.00266	13.94	0.0010
Pilots/GS angle/Offset	0.00075	2	0.00038	1.98	0.1606
Error	0.00458	24	0.00019		

TABLE II. Continued

Separation - 60 sec/4.5 deg GS angle

Cell means for first dependent variable

Pilots =	Pilot1	Pilot1	Pilot2	Pilot2	Pilot3	Pilot3	marginal
Vref =	same	higher	same	higher	same	higher	
Separation	2.36667	2.35000	2.37333	2.35000	2.37000	2.35500	2.36542
count	6	2	6	2	6	2	24

Standard deviations for first dependent variable

Pilots =	Pilot1	Pilot1	Pilot2	Pilot2	Pilot3	Pilot3
Vref =	same	higher	same	higher	same	higher
Separation	0.00816	0.00000	0.02658	0.01414	0.00632	0.00707

Analysis of variance for first
dependent variable - Separation

source	sum of squares	degrees of freedom	mean square	f	tail probability
Mean	100.32361	1	100.32361	418337.84	0.0000
Pilots	0.00006	2	0.00003	0.12	0.8862
Vref	0.00151	1	0.00151	6.31	0.0218
Interaction	0.00006	2	0.00003	0.12	0.8862
Error	0.00432	18	0.00024		

TABLE II. Continued

Glide-Slope Error - 60 sec separation/same Vref

Cell means for first dependent variable

Pilots =	Pilot1	Pilot1	Pilot1	Pilot1	Pilot2	Pilot2	Pilot2	Pilot2
GS angle=	3 degree	3 degree	4.5 degree	4.5 degree	3 degree	3 degree	4.5 degree	4.5 degree
Offset =	none	offset	none	offset	none	offset	none	offset
GS error	0.00667	0.01167	0.00840	0.00837	0.04021	0.01480	0.02112	0.01914
count	3	3	3	3	3	3	3	3

Pilots =	Pilot3	Pilot3	Pilot3	Pilot3	marginal
GS angle=	3 degree	3 degree	4.5 degree	4.5 degree	
Offset =	none	offset	none	offset	
GS error	-0.01098	-0.00994	-0.00328	-0.00166	0.00871
count	3	3	3	3	36

Standard deviations for first dependent variable

Pilots =	Pilot1	Pilot1	Pilot1	Pilot1	Pilot2	Pilot2	Pilot2	Pilot2
GS angle=	3 degree	3 degree	4.5 degree	4.5 degree	3 degree	3 degree	4.5 degree	4.5 degree
Offset =	none	offset	none	offset	none	offset	none	offset
GS error	0.00523	0.00577	0.02367	0.01331	0.00685	0.01009	0.00781	0.00371

Pilots =	Pilot3	Pilot3	Pilot3	Pilot3
GS angle=	3 degree	3 degree	4.5 degree	4.5 degree
Offset =	none	offset	none	offset
GS error	0.00140	0.00219	0.00299	0.00158

Analysis of variance for first
dependent variable - glide-slope error

source	sum of squares	degrees of freedom	mean square	f	tail probability
Mean	0.00273	1	0.00273	31.54	0.0000
Pilots	0.00550	2	0.00275	31.76	0.0000
GS angle	0.00000	1	0.00000	0.00	0.9849
Offset	0.00010	1	0.00010	1.13	0.2987
Pilot/GS angle	0.00036	2	0.00018	2.06	0.1496
Pilot/Offset	0.00049	2	0.00024	2.82	0.0794
GS angle/Offset	0.00009	1	0.00009	1.04	0.3179
Pilot/GS angle/Offset	0.00034	2	0.00017	1.97	0.1617
Error	0.00208	24	0.00009		

TABLE II. Continued

Glide-Slope Error - excluding run 47

Cell means for first dependent variable

Pilots =	Pilot1	Pilot1	Pilot1	Pilot1	Pilot2	Pilot2	Pilot2	Pilot2
GS angle=	3 degree	3 degree	4.5 degree	4.5 degree	3 degree	3 degree	4.5 degree	4.5 degree
Offset =	none	offset	none	offset	none	offset	none	offset
GS error	0.00667	0.01167	0.00880	0.01828	0.04021	0.01480	0.02632	0.02085
count	3	3	5	6	3	3	5	6

Pilots =	Pilot3	Pilot3	Pilot3	Pilot3	marginal
GS angle=	3 degree	3 degree	4.5 degree	4.5 degree	
Offset =	none	offset	none	offset	
GS error	-0.01098	-0.00994	-0.00273	-0.00138	0.01097
count	3	3	4	6	50

Standard deviations for first dependent variable

Pilots =	Pilot1	Pilot1	Pilot1	Pilot1	Pilot2	Pilot2	Pilot2	Pilot2
GS angle=	3 degree	3 degree	4.5 degree	4.5 degree	3 degree	3 degree	4.5 degree	4.5 degree
Offset =	none	offset	none	offset	none	offset	none	offset
GS error	0.00523	0.00577	0.01678	0.01481	0.00685	0.01009	0.01270	0.01237

Pilots =	Pilot3	Pilot3	Pilot3	Pilot3
GS angle=	3 degree	3 degree	4.5 degree	4.5 degree
Offset =	none	offset	none	offset
GS error	0.00140	0.00219	0.00267	0.00337

Analysis of variance for first
dependent variable - glide-slope error

source	sum of squares	degrees of freedom	mean square	f	tail probability
Mean	0.00477	1	0.00477	43.75	0.0000
Pilots	0.00767	2	0.00383	35.15	0.0000
GS angle	0.00010	1	0.00010	0.91	0.3459
Offset	0.00006	1	0.00006	0.57	0.4537
Pilot/GS angle	0.00030	2	0.00015	1.38	0.2647
Pilot/Offset	0.00107	2	0.00053	4.88	0.0129
GS angle/Offset	0.00019	1	0.00019	1.78	0.1900
Pilot/GS angle/Offset	0.00020	2	0.00010	0.94	0.4008
Error	0.00414	38	0.00011		

TABLE II. Continued

Glide-Slope Error

Cell means for first dependent variable

Pilots =	Pilot1	Pilot1	Pilot1	Pilot1	Pilot2	Pilot2	Pilot2	Pilot2
GS angle=	3 degree	3 degree	4.5 degree	4.5 degree	3 degree	3 degree	4.5 degree	4.5 degree
Offset =	none	offset	none	offset	none	offset	none	offset
GS error	0.00667	0.01167	0.00880	0.01828	0.04021	0.01480	0.02632	0.02085
count	3	3	5	6	3	3	5	6

Pilots =	Pilot3	Pilot3	Pilot3	Pilot3	marginal
GS angle=	3 degree	3 degree	4.5 degree	4.5 degree	
Offset =	none	offset	none	offset	
GS error	-0.01098	-0.00994	0.03166	-0.00138	0.01407
count	3	3	5	6	51

Standard deviations for first dependent variable

Pilots =	Pilot1	Pilot1	Pilot1	Pilot1	Pilot2	Pilot2	Pilot2	Pilot2
GS angle=	3 degree	3 degree	4.5 degree	4.5 degree	3 degree	3 degree	4.5 degree	4.5 degree
Offset =	none	offset	none	offset	none	offset	none	offset
GS error	0.00523	0.00577	0.01678	0.01481	0.00685	0.01009	0.01270	0.01237

Pilots =	Pilot3	Pilot3	Pilot3	Pilot3
GS angle=	3 degree	3 degree	4.5 degree	4.5 degree
Offset =	none	offset	none	offset
GS error	0.00140	0.00219	0.07694	0.00337

Analysis of variance for first
dependent variable - glide-slope error

source	sum of squares	degrees of freedom	mean square	f	tail probability
Mean	0.00795	1	0.00795	11.15	0.0019
Pilots	0.00424	2	0.00212	2.97	0.0628
GS angle	0.00088	1	0.00088	1.23	0.2747
Offset	0.00076	1	0.00076	1.06	0.3093
Pilot/GS angle	0.00179	2	0.00090	1.26	0.2953
Pilot/Offset	0.00136	2	0.00068	0.95	0.3939
GS angle/Offset	0.00003	1	0.00003	0.04	0.8382
Pilot/GS angle/Offset	0.00150	2	0.00075	1.05	0.3594
Error	0.02780	39	0.00071		

TABLE II. Concluded

Localizer Error

Cell means for first dependent variable

Pilots =	Pilot1	Pilot1	Pilot1	Pilot1	Pilot2	Pilot2	Pilot2	Pilot2
GS angle=	3 degree	3 degree	4.5 degree	4.5 degree	3 degree	3 degree	4.5 degree	4.5 degree
Offset =	none	offset	none	offset	none	offset	none	offset
LOC error	0.14221	0.15594	-0.01864	0.00062	0.13803	0.13264	0.00988	-0.07092
count	3	3	5	6	3	3	5	6

Pilots =	Pilot3	Pilot3	Pilot3	Pilot3	marginal
GS angle=	3 degree	3 degree	4.5 degree	4.5 degree	
Offset =	none	offset	none	offset	
LOC error	0.17049	0.11465	0.04829	0.04992	0.05171
count	3	3	5	6	51

Standard deviations for first dependent variable

Pilots =	Pilot1	Pilot1	Pilot1	Pilot1	Pilot2	Pilot2	Pilot2	Pilot2
GS angle=	3 degree	3 degree	4.5 degree	4.5 degree	3 degree	3 degree	4.5 degree	4.5 degree
Offset =	none	offset	none	offset	none	offset	none	offset
LOC error	0.04367	0.05767	0.06795	0.06648	0.01553	0.03818	0.06640	0.10341

Pilots =	Pilot3	Pilot3	Pilot3	Pilot3
GS angle=	3 degree	3 degree	4.5 degree	4.5 degree
Offset =	none	offset	none	offset
LOC error	0.01439	0.10133	0.03383	0.04890

Analysis of variance for first dependent variable - localizer error

source	sum of squares	degrees of freedom	mean square	f	tail probability
Mean	0.24591	1	0.24591	58.83	0.0000
Pilots	0.01477	2	0.00739	1.77	0.1842
GS angle	0.22480	1	0.22480	53.78	0.0000
Offset	0.00372	1	0.00372	0.89	0.3512
Pilot/GS angle	0.01223	2	0.00611	1.46	0.2440
Pilot/Offset	0.00736	2	0.00368	0.88	0.4225
GS angle/Offset	0.00005	1	0.00005	0.01	0.9137
Pilot/GS angle/Offset	0.00868	2	0.00434	1.04	0.3636
Error	0.16301	39	0.00418		

TABLE III. QUESTIONNAIRE RESPONSE

[The following results are the normalized values of the pilot responses to the questionnaire of appendix A]

(a) Horizontal-path tracking task

<table>
<tr><th>Test condition</th><th colspan="2">No noticeable work load</th><th colspan="2">Very easy</th><th colspan="2">Easy</th><th colspan="2">Some effort required</th><th>Impossible</th></tr>
<tr><td>All 3° glide slope</td><td colspan="2">16%</td><td colspan="2">39%</td><td colspan="2">39%</td><td colspan="2">6%</td><td></td></tr>
<tr><td>All 4.5° glide slope</td><td colspan="2">6%</td><td colspan="2">58%</td><td colspan="2">14%</td><td colspan="2">22%</td><td></td></tr>
<tr><td>All without offset</td><td colspan="2">11%</td><td colspan="2">50%</td><td colspan="2">22%</td><td colspan="2">17%</td><td></td></tr>
<tr><td>All with offset</td><td colspan="2">11%</td><td colspan="2">47%</td><td colspan="2">31%</td><td colspan="2">11%</td><td></td></tr>
<tr><td>4.5° glide slope with offset (1)[a]</td><td></td><td></td><td>56%</td><td>67%</td><td>22%</td><td>11%</td><td>22%</td><td>22%</td><td></td></tr>
<tr><td>4.5° glide slope without offset (2)[a]</td><td>11%</td><td>17%</td><td>56%</td><td>50%</td><td>11%</td><td></td><td>22%</td><td>33%</td><td></td></tr>
</table>

[a]Explanation of pilot work-load ratings is given as follows:

Data-block format (1)

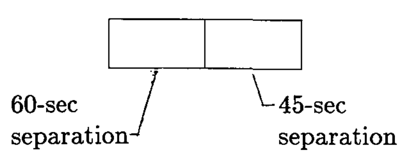

Data-block format (2)

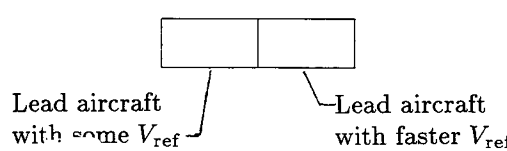

TABLE III. Continued

(b) Vertical-path tracking task

Test condition	No noticeable work load		Very easy		Easy		Some effort required		Impossible
All 3° glide slope	17%		44%		22%		17%		
All 4.5° glide slope	6%		50%		17%		27%		
All without offset	11%		50%		14%		25%		
All with offset	11%		44%		25%		20%		
4.5° glide slope with offset (1)[a]			56%	56%	11%	22%	33%	22%	
4.5° glide slope without offset (2)[a]	11%	17%	56%	33%	11%	17%	22%	33%	

[a]Explanation of pilot work-load ratings is given as follows:

Data-block format (1)

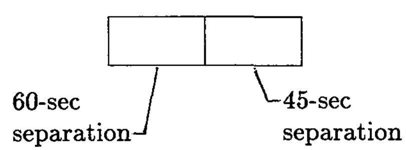

Data-block format (2)

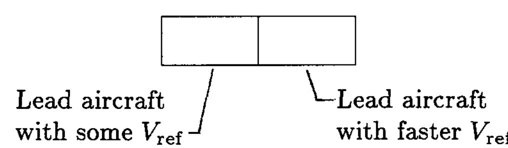

TABLE III. Concluded

(c) Self-separation task

Test condition	No noticeable work load	Very easy		Easy		Some effort required		Impossible
All 3° glide slope	6%	55%		33%		6%		
All 4.5° glide slope		52%		31%		17%		
All without offset		64%		25%		11%		
All with offset	6%	44%		39%		11%		
4.5° glide slope with offset (1)[a]		56%	33%	22%	45%	22%	22%	
4.5° glide slope without offset (2)[a]		56%	67%	33%	33%	11%		

[a]Explanation of pilot work-load ratings is given as follows:

Data-block format (1)

60-sec separation | 45-sec separation

Data-block format (2)

Lead aircraft with some V_{ref} | Lead aircraft with faster V_{ref}

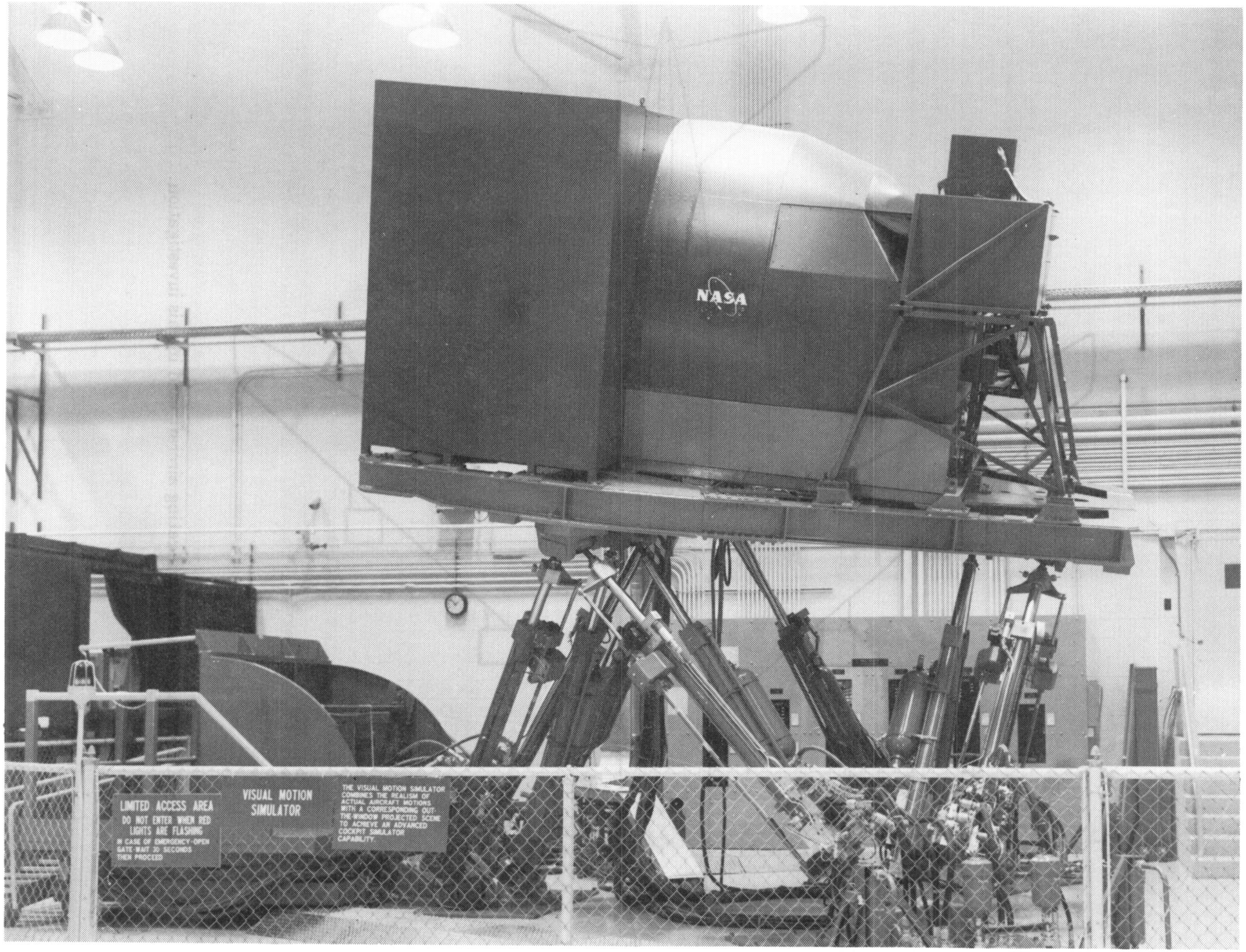

L-74-5843

Figure 1. The Langley Visual/Motion Simulator.

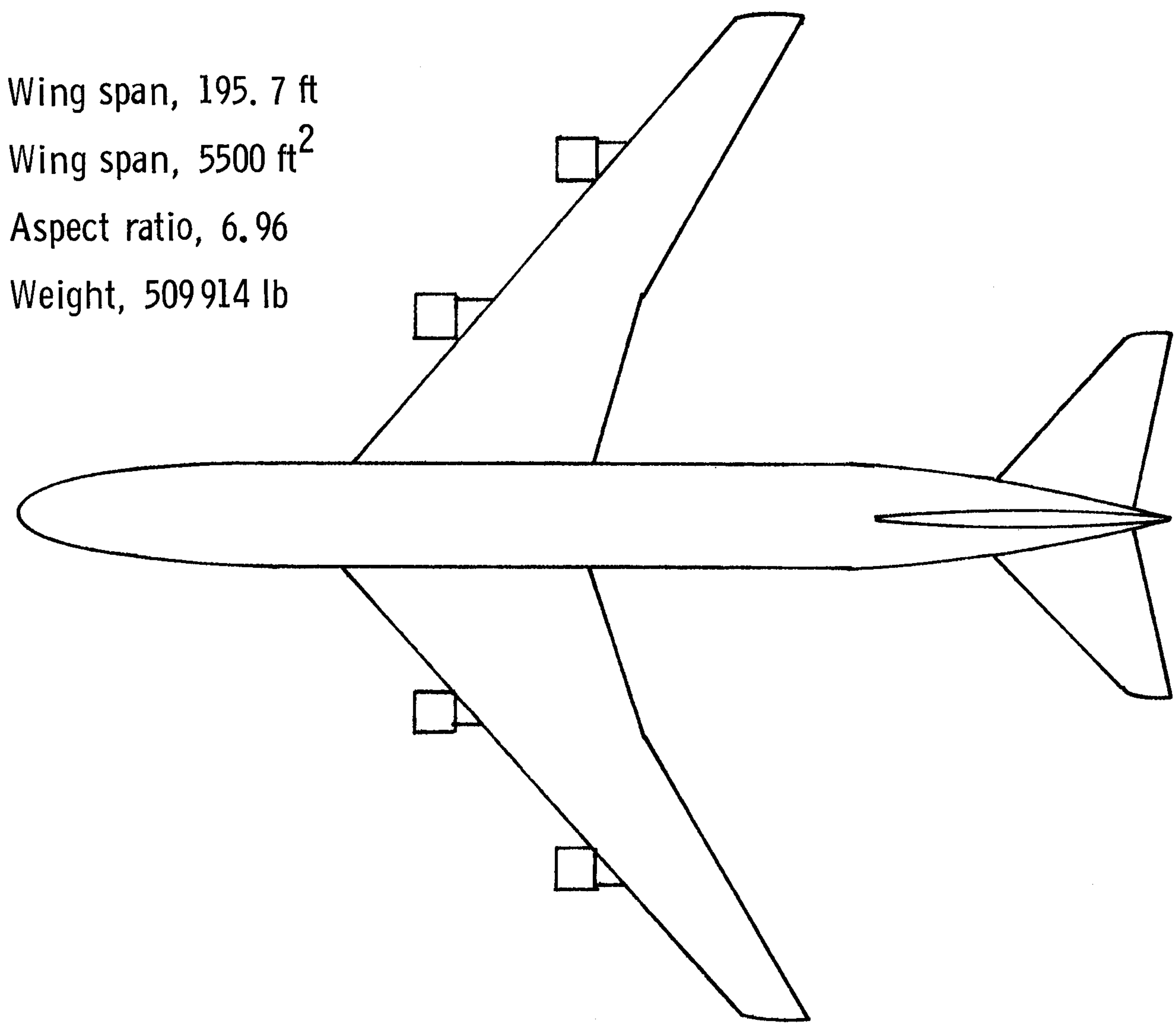

Figure 2. Drawing of vortex-generating aircraft used in this investigation.

L-75-7496

Figure 3. Visual landing display system at the Langley Research Center.

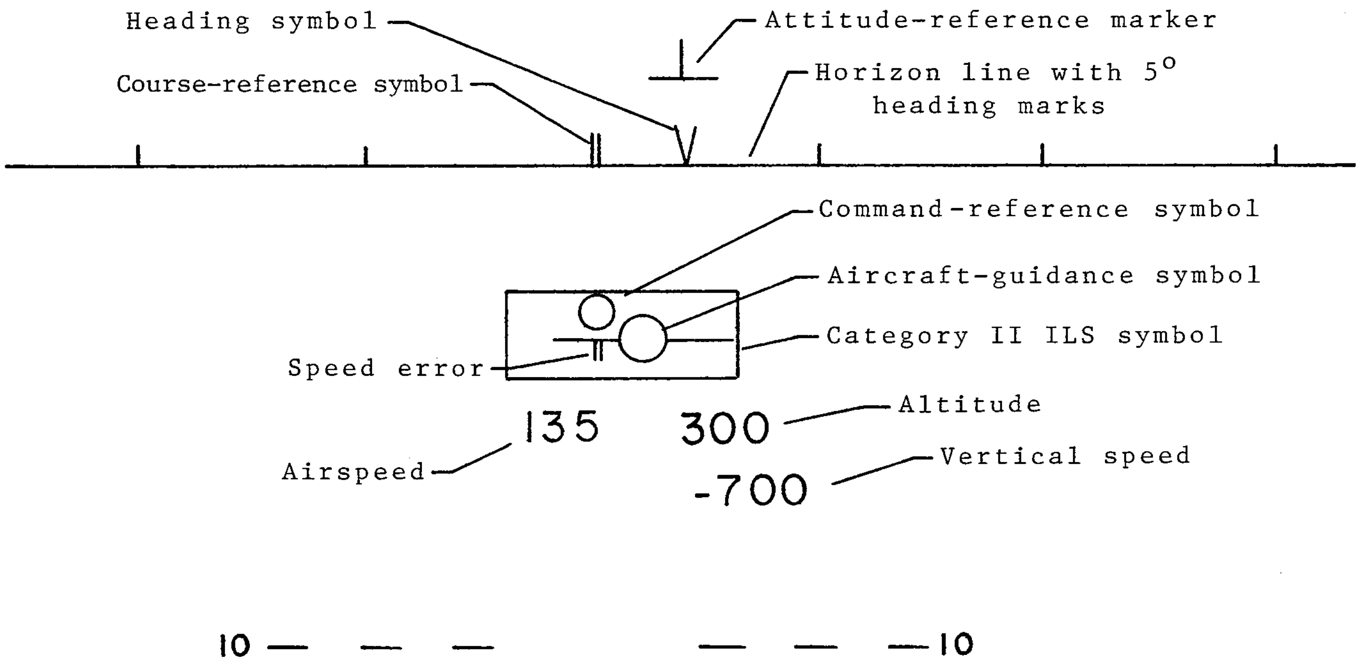

The conditions shown are as follows:

- 2° pitch attitude
- 2° right drift-correction angle
- 135-knot airspeed
- 300-ft altitude
- 700-ft/min descent
- Within the category II ILS limits (slightly low and to right)
- 3 knots slow
- Pitch-up and roll-left command

Figure 4. Basic-display format.

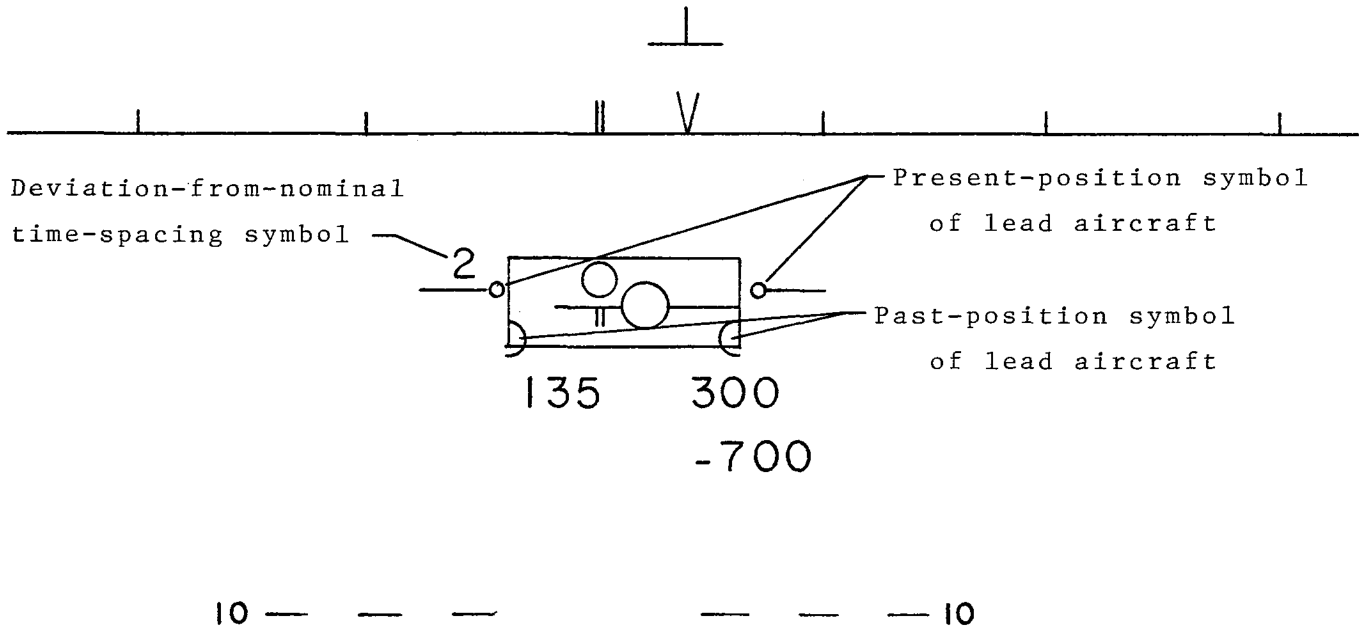

The conditions shown are as follows:

- Leader is slightly high on the ILS.
- Leader was slightly low on the ILS.
- 2-sec slow separation error

Figure 5. Traffic-display format.

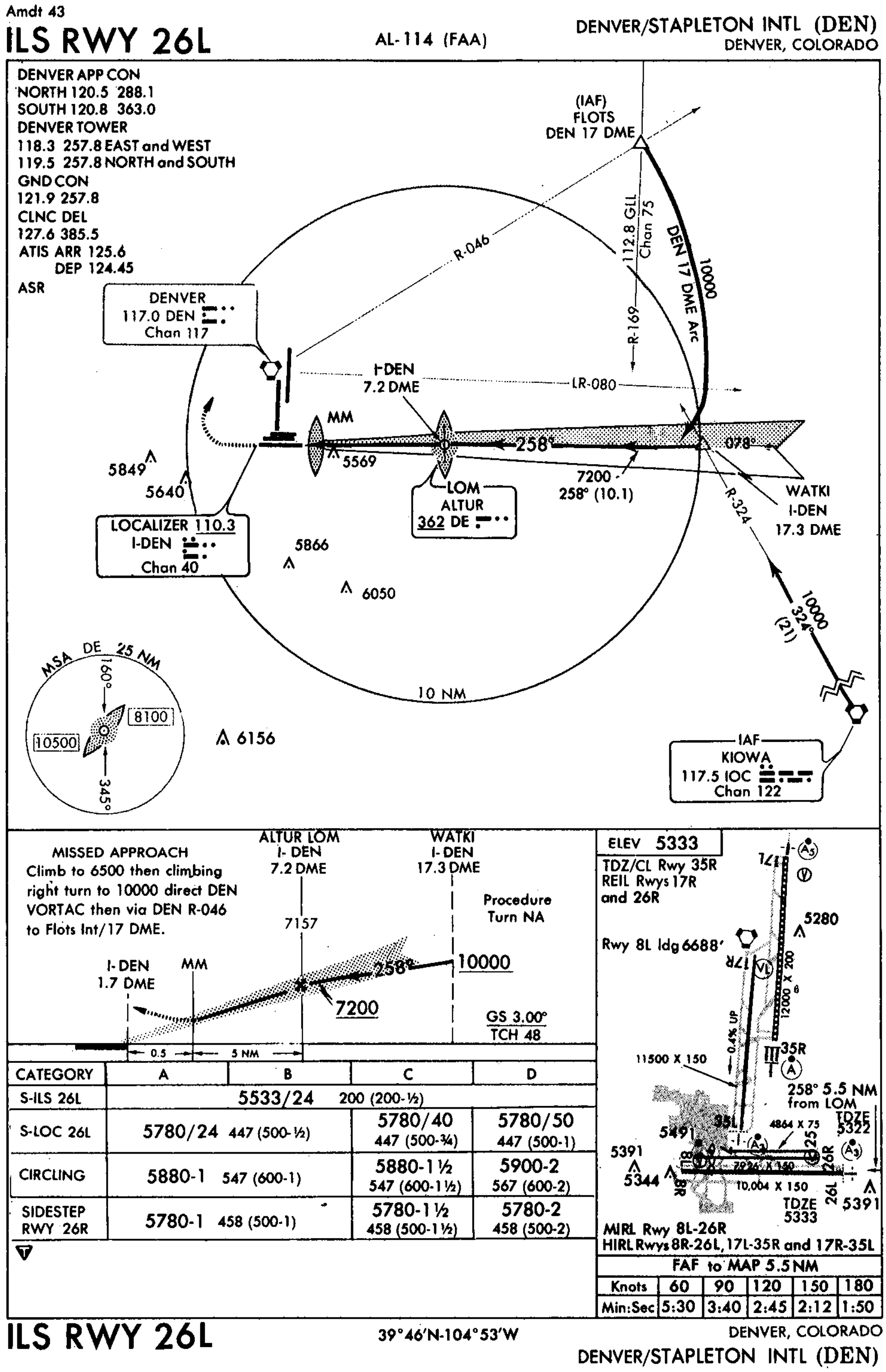

Figure 6. Sample approach chart. Decision height was reduced to 150 ft for this study.

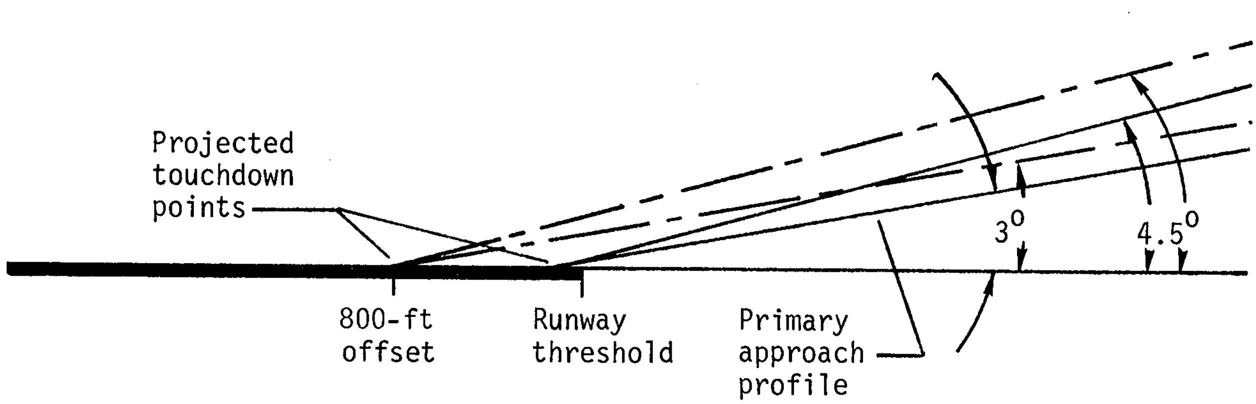

Figure 7. Illustration of four approach profiles utilized by ownship.

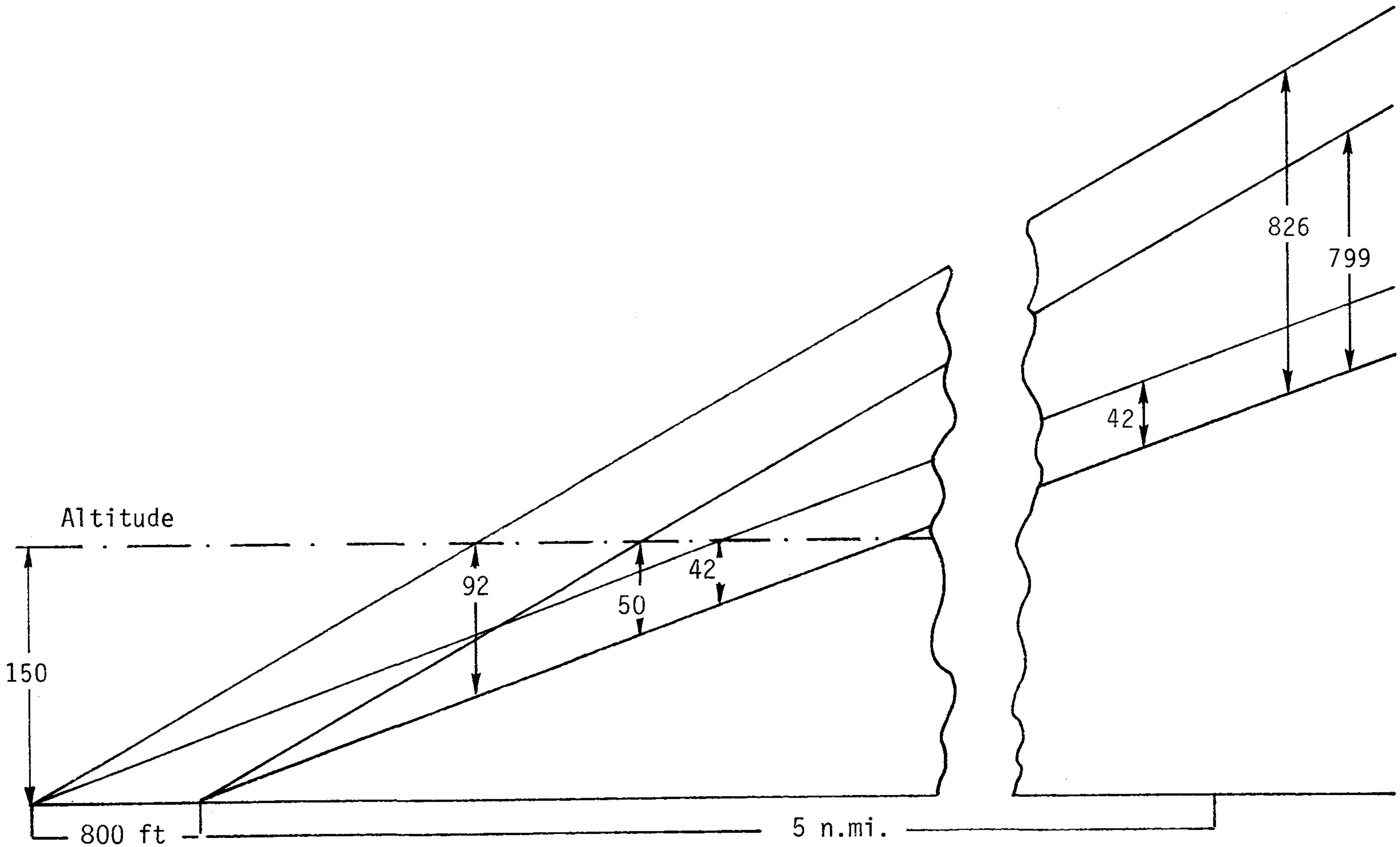

Figure 8. Vertical-path separation at 150 ft in altitude and at 5 n.mi. in range. All dimensions are given in feet unless otherwise specified.

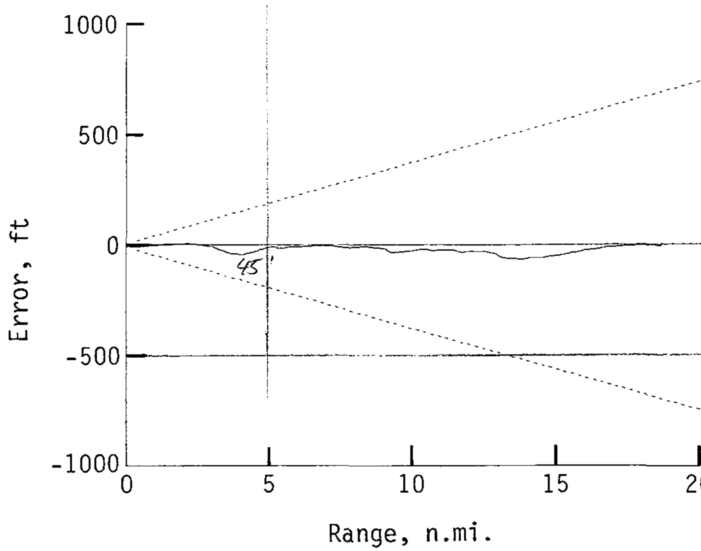

(a) Glide-slope error of traffic profile 1.

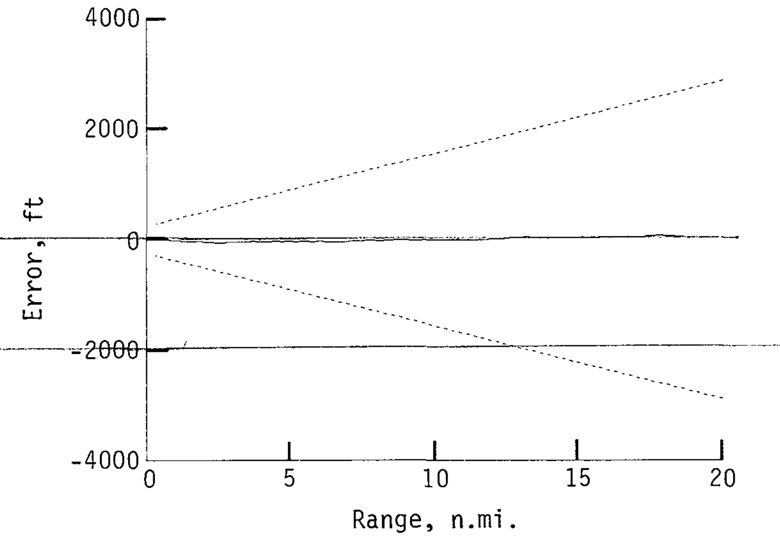

(b) Localizer error of traffic profile 1.

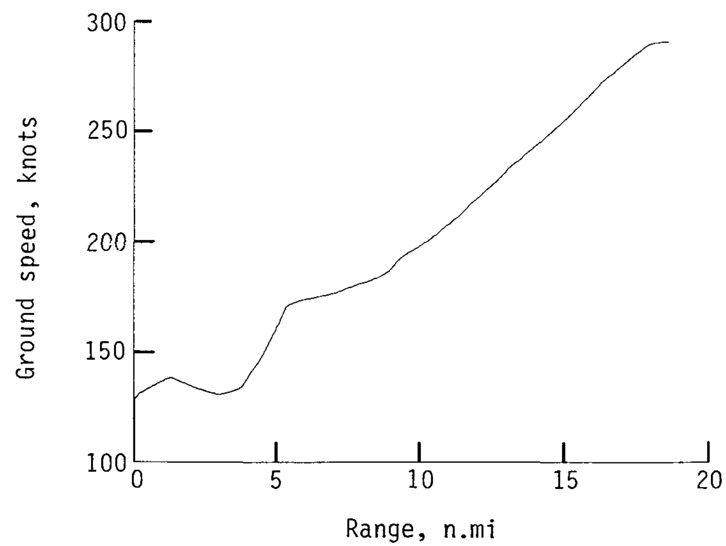

(c) Ground speed of traffic profile 1.

Figure 9. Flight-path performance of traffic profiles 1 and 2. Dashed lines indicate category II ILS window edges.

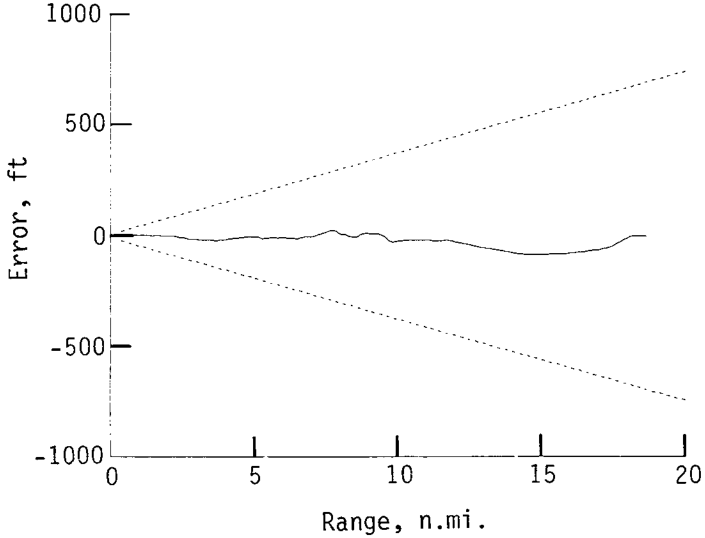

(d) Glide-slope error of traffic profile 2.

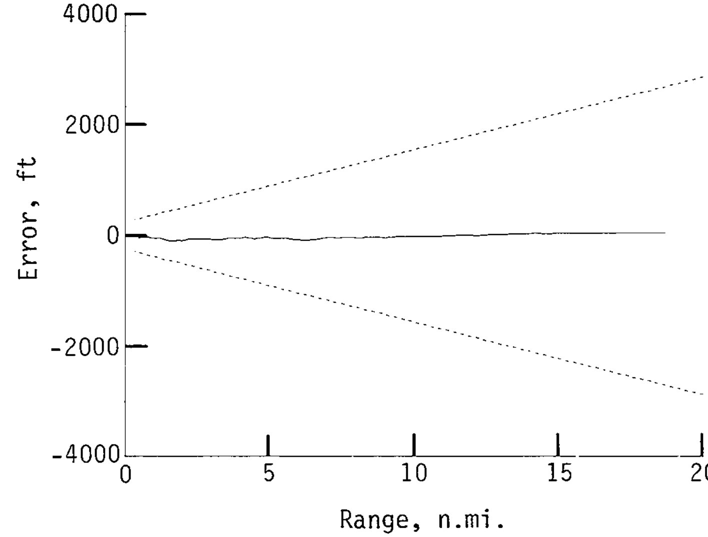

(e) Localizer error of traffic profile 2.

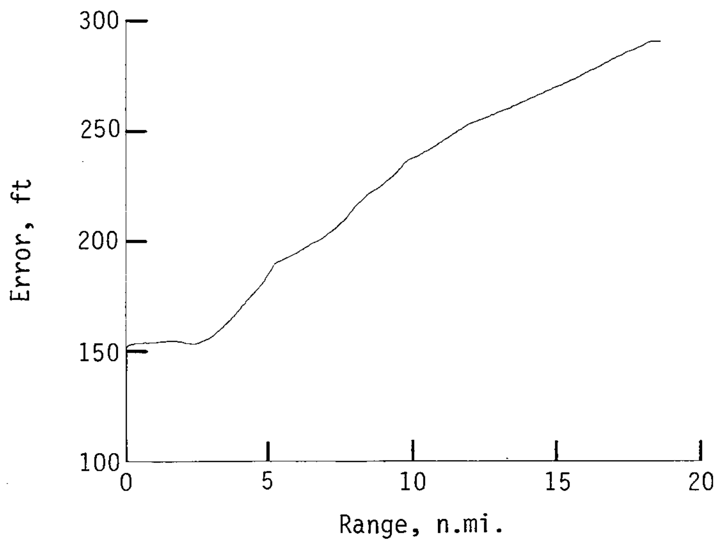

(f) Ground speed of traffic profile 2.

Figure 9. Concluded.

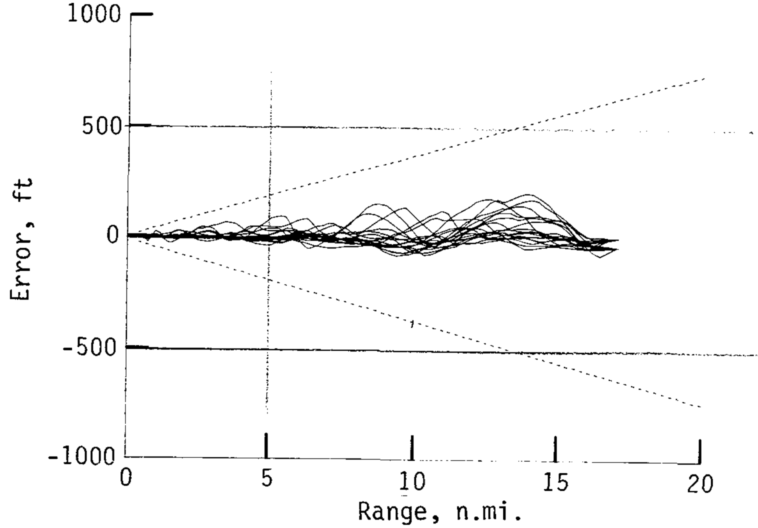

(a) Glide-slope error for 3° glide-slope approaches.

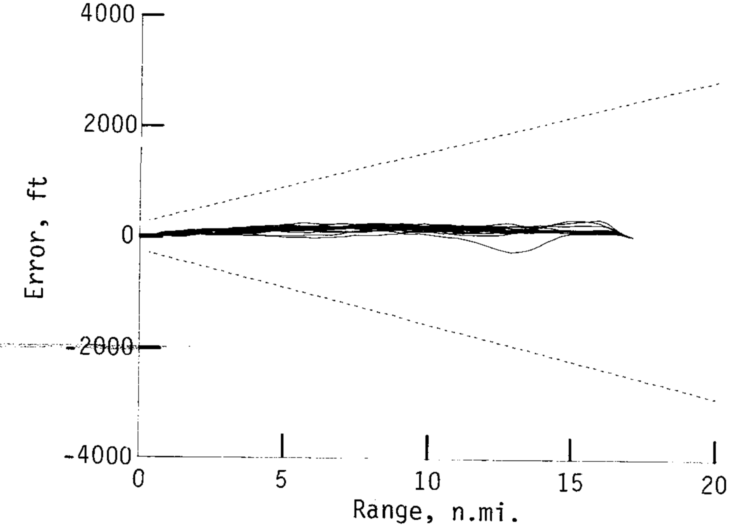

(b) Localizer error for 3° glide-slope approaches.

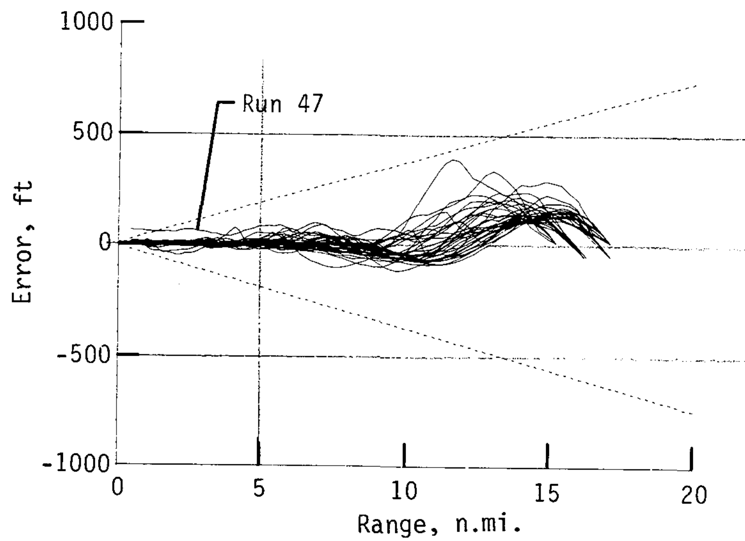

(c) Glide-slope error for 4.5° glide-slope approaches.

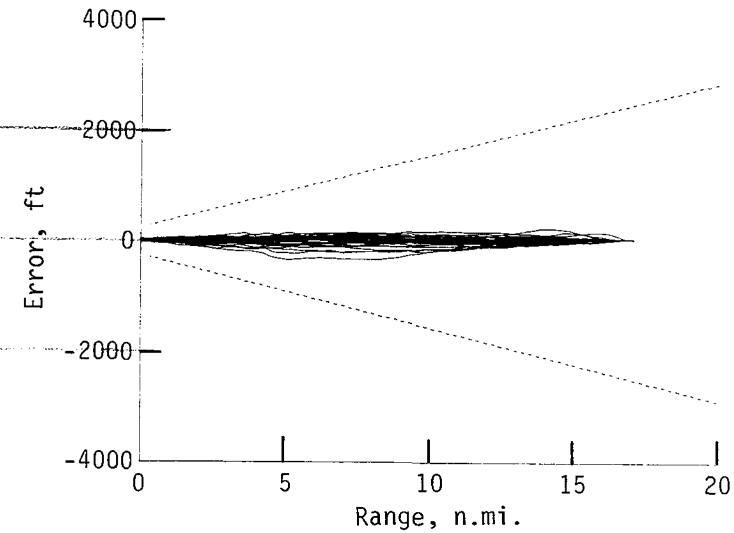

(d) Localizer error for 4.5° glide-slope approaches.

Figure 10. ILS tracking performance. Dashed lines indicate category II ILS window edges.

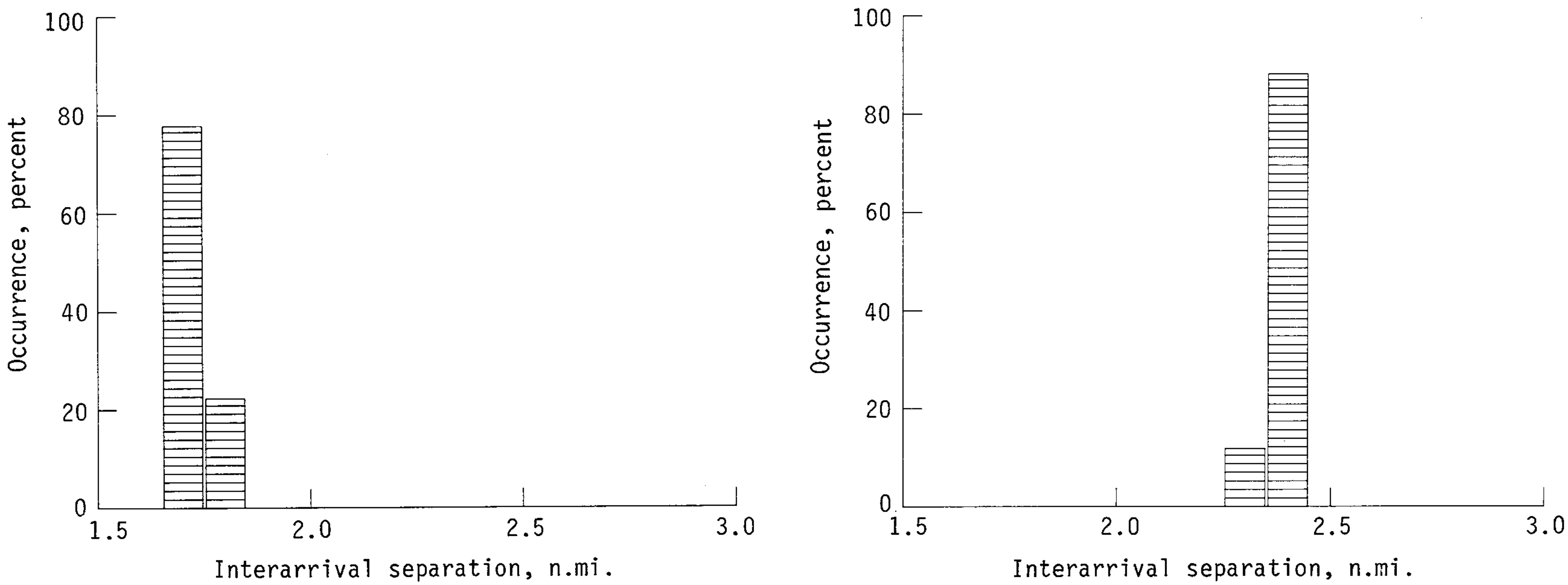

(a) 45-sec separation.

(b) 60-sec separation.

Figure 11. Interarrival separation results.

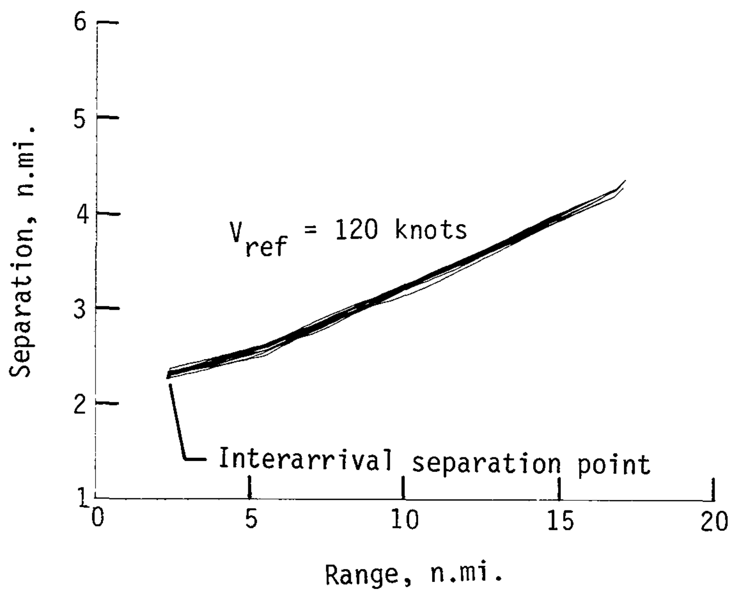

(a) In-trail separation for 3° glide-slope approaches.

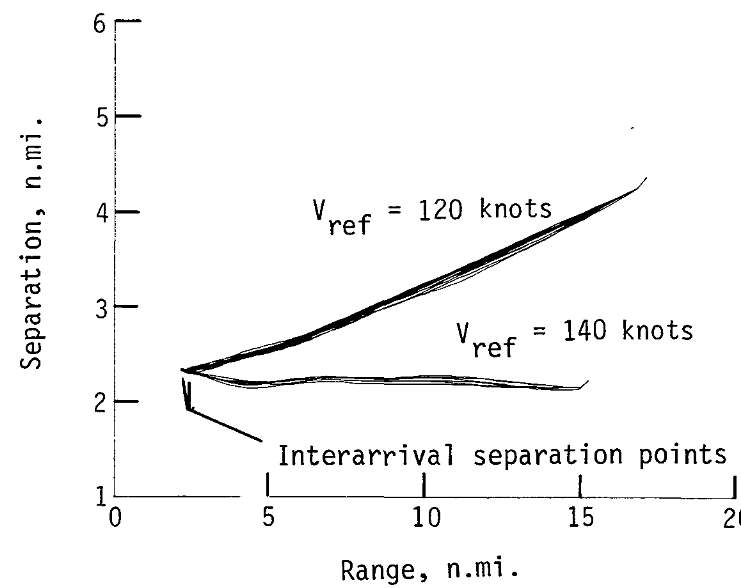

(b) In-trail separation for 4.5° glide-slope approaches.

Figure 12. In-trail separation intervals. V_{ref} speeds are for lead aircraft.

1. Report No. NASA TP-2386	2. Government Accession No.	3. Recipient's Catalog No.
4. Title and Subtitle A COCKPIT-DISPLAY CONCEPT FOR EXECUTING A MULTIPLE GLIDE-SLOPE APPROACH FOR WAKE-VORTEX AVOIDANCE		5. Report Date February 1985
		6. Performing Organization Code 505-35-13-05
7. Author(s) Terence S. Abbott		8. Performing Organization Report No. L-15852
9. Performing Organization Name and Address NASA Langley Research Center Hampton, VA 23665		10. Work Unit No.
		11. Contract or Grant No.
12. Sponsoring Agency Name and Address National Aeronautics and Space Administration Washington, DC 20546		13. Type of Report and Period Covered Technical Paper
		14. Sponsoring Agency Code

15. Supplementary Notes

16. Abstract

A piloted simulation study was undertaken to determine the feasibility of utilizing a forward-looking display to provide information that would enable aircraft to reduce their in-trail separation interval, and hence increase airport capacity, through the application of multiple glide-path approach techniques. The primary objective of this study was to determine whether information could be satisfactorily provided on a head-up display (HUD) format to permit the pilot to conduct a multiple glide-slope approach while maintaining a prespecified in-trail separation interval. The tests were conducted in a motion-base cockpit simulator configured as a current-generation transport aircraft and included dynamic effects of the vortices generated by the lead aircraft. The information provided on the HUD included typical aircraft guidance information and the current and past positions of the lead aircraft. Additionally, the displayed information provided self-separation cues that allowed the pilot to maintain separation on the lead aircraft. Performance data and pilot subjective ratings and comments were obtained during the tests. The results of this study indicate that multiple glide-slope approaches, procedurally designed for vortex avoidance, are possible while maintaining pilot work load and performance within operationally acceptable limits. In general, then, it would seem that multiple glide-slope approaches are possible even under reduced in-trail separation conditions if the pilot is provided with adequate situational information.

17. Key Words (Suggested by Authors(s))	18. Distribution Statement
Cockpit display Air Traffic Control Aircraft guidance Data links	Unclassified—Unlimited Subject Category 06

19. Security Classif.(of this report)	20. Security Classif.(of this page)	21. No. of Pages	22. Price
Unclassified	Unclassified	42	A03

For sale by the National Technical Information Service, Springfield, Virginia 22161

National Aeronautics and
Space Administration

Washington, D.C.
20546

Official Business
Penalty for Private Use, $300

THIRD-CLASS BULK RATE

Postage and Fees Paid
National Aeronautics and
Space Administration
NASA-451

U.S.MAIL

NASA

POSTMASTER: If Undeliverable (Section 158 Postal Manual) Do Not Return

DO NOT REMOVE SLIP FROM MATERIAL

Delete your name from this slip when returning material to the library.

NAME	MS
James Ferris	294
~~R. Stoever~~	~~217~~

NASA Langley (Rev. May 1988) RIAD N-75